Determination of electrochemical active surface area of different physicochemical surfaces

Worapot Prongmanee[1 a], Piyapong Asanithi[1, 2, 3, b]

[1] Department of Physics, Faculty of Science, King Mongkut's University of Technology Thonburi, Bangkok, 10140, Thailand.

[2] ThEP Center, Commission of Higher Education, 328 Si Ayuthaya Rd., Thailand.

[3] Theoretical and Computational Science Center (TaCS), Science Laboratory Building, Faculty of Science, King Mongkut's University of Technology Thonburi, Bangkok, 10140, Thailand.

[a] <worapot.nano@mail.kmutt.ac.th>, [b] piyapong.asa@mail.kmutt.ac.th

Abstract

Determination of electrochemical active surface area (EAS) of materials is essential for many applications, including electrochemical electrode fabrication, biosensor, catalytic activity, etc. There are few electrochemical techniques using to determine EAS, including cyclic voltammetry (CV), chronoamperometry (CH-AMP) and chronocoulometry (CH-COU). However, most of them are reported separately as single technique. In this report, we aim to determine EAS of materials having different physicochemical surfaces based on CV, CH-AMP and CH-COU. The EAS of each material obtained from CV, CH-AMP and CH-COU are compared and discussed. The materials include bare screen-printed electrode (bare@SP, rough and hydrophobic surface), graphene oxide modified SP (GO@SP, smooth and hydrophilic surface) and hydroxyapatite-graphene oxide composite modified SP (HAp-GO@SP, rough and hydrophilic surface). 10 mM $[Fe(CN)_6]^{-4/-3}$ in 0.1 M KCl was used as an electrolyte. Physical and chemical properties of materials were determined by contract angle measurement and scanning electron microscope. The results show that the above-mentioned techniques provide dissimilar EAS values. We also find out that the ESA of bare@SP is higher than those of HAp-GO@SP and GO@SP in 10 mM $[Fe(CN)_6]^{-4/-3}$ in 0.1 M KCl. Furthermore, ESA values obtained from CV is higher than those of CH-AMP and CH-COU, respectively.

Keywords: *cyclic voltammetry, chronoamperometry, chronocoulometry, Electrochemical active surface area, screen-printed electrode, physicochemical surface*

1. Introduction

Electrochemical active surface area (EAS) is important for electrochemical research such as super capacitor [1], photovoltaic device [2], fuel cell electrode [3, 4], biosensor [5], catalytic application [6]. The EAS can be used as an indicator to evaluate the electrochemical performance of electrode material, such as charge transfer, double layer capacitance and actual active area interface between active species and surface of material [7]. Generally, determination of physical surface area (PSA) can be performed by nitrogen adsorption based on the Brunauer Emmett and Teller (BET) technique [1, 8, 9]. The sample

for BET measurement needs to be dried powder to provide significant signal. Wetted samples and agglomerated samples may be not possible. Moreover, BET cannot evaluate the surface area of electrode material in the presence of electrolyte species. Some materials provide high PSA, but low ESA which may not be good for applications in electrochemistry. In contrast, materials with low PSA may provide high ESA, which is useful for many electrochemical applications. Thus, measuring ESA can be examined with electrochemical approaches, including cyclic voltammetry (CV), chronoamperometry (CH-AMP) and chronocoulometry (CH-COU).

Cyclic voltammetry (CV) is a general technique to provide electrochemical information of electrode material and electrolyte species. The sweep potential of linear triangular waveform provides the information about location of potential of redox reaction of analytic species, charge transfer reaction or adsorption process. From CV result, the relationship between electrochemical peak currents and peak potentials from oxidation-reduction reactions is obtained as a cyclic voltammogram [10]. Information obtained from cyclic voltammogram can be used to evaluate the ESA based on Randle-Sevcik equation [11, 12, 13]. The slope of the linear correlation of the plot between peak current (y axis) and square root of scan rate (x axis) can be used for determination of the ESA.

Chronoamperometry (CH-AMP) is a technique that the applied potential is fixed at a constant value. The electrochemical current is recorded from no reaction until occurring reaction of electroactive species related to fixed applied potential. The CH-AMP results displays as a plot between current and time. This plot provides information relating to the diffusion coefficient of the analytic species and the ESA. The slope of the plot can be used for determination of ESA based on Cottrel equation [10].

Chronoamperometry (CH-COU) is a developed technique of CH-AMP. Although CH-COU is similar to CH-AMP for using in electrochemical measurement, it gives accurately parameter from calculation such as kinetic rate constant and monitoring adsorption of analyzed species on electrode interface. The accurate determination is due to the integration of recorded current, fixed applied potential and recorded charges including electrical double layer and adsorbed analyzed species on electrode. CH-COU can be used to evaluate the ESA in electrochemical sensor [15, 16]. The CH-COU reveal relationship between charge and time and the ESA can be calculated based on the Anson equation [17]. Slope found in plot of charge versus square root of time can be used to estimate the ESA.

However, in general, the ESA is always calculated by individual techniques as above-mentioned. This work proposed to determine and compare the ESA based on these three techniques. The effects of physicochemical characteristics of material electrodes, including hydrophobicity and surface roughness on the ESA values obtained from each technique were reported and discussed. All samples were measured in ferricyanide ion $[Fe(CN)_6]^{-4/-3}$ contained in potassium chloride (KCl).

2. Experiment setup

2.1 Preparation of bare@SP, GO@SP and HAp-GO@SP

The screen-printed electrode (SP, CI1730OR) from Quasense was employed in this experiment. The reference electrode (RE), counter electrode (CE) and working electrode were fabricated from carbon, silver/silver chloride and carbon, respectively. SP was rinsed by deionized water (DI-water) and dried in air. The WE (0.071 cm^2 in area) was coated by 2 µL of GO suspension (3.13 mg/mL) and dried in hot air oven at 45 ºC for 15 min in graphene oxide modified SP (GO@SP). For preparation of hydroxyapatite-graphene oxide composite modified SP (HAp-GO@SP), 2 µL solution of suspension of HAp-GO (3.25 mg/mL) was employed in preparation following procedure of HAp-GO@SP.

2.2 Contact angle measurement and investigation of surface morphology of electrode surface

The contact angle measurement was carried out by dropping 1 µL DI-water on bare@SP GO@SP and HAp-GO@SP at room temperature. The contact angle meter (SL150, Kino) was operated in this study. For morphological investigation, these samples were observed via scanning electron microscope (SEM, JSM-6610 LV, JEOL). The condition of SEM was operated at acceleration voltage 10 kV under vacuum.

2.3 Electrochemical setup of determination of ESA in ferricyanide

Electrochemical setups used potentiostat (VersaSTAT4, Princeton Applied Research), which was connected screen-printed electrode via boxed connector (DSC, Dropsense). 200 µL of 10 mM $K_3[Fe(CN_3)_6]$ in 0.1 M KCl were dropped on SP to cover CE, RE and WE area. The experiments were accomplished at room temperature. Cyclic voltammetry (CV) was operated at potential between -0.5 V to 0.5 V. The scan rates were adjusted at 10, 30, 50, 80 and 100 $mV \cdot S^{-1}$. Both of chronoamperometry (CH-AMP) and chronocoulometry (CH-COU) were monitoring at an applied potential of 0.27 V.

3. Results and discussion

3.1 Surface characterization of bare@SP, GO@SP and HAp-GO@SP

The morphological surface of working electrode (WE) of bare@SP was investigated via SEM. Figure 1 (a) revealed the roughness of WE area as a result of blending of both flake and powder carbon black [18]. Next, the GO and HAp-GO suspension coated on WE showed perfect coating. The investigation of their surface exposed the smooth layer of GO coated on roughness of bare electrode as shown in Figure 2 (b), while HAp-GO (Figure 1 (c)) showed rough surface because of unification of HAp particles (2-3 in diameter) and GO layer. The physicochemical surfaces regarding wettability were investigated by contact angle. Insets of Figures 1 (a-c) showed the contact angle of 1 µL of a DI-water drop on

different electrodes. The carbon black on WE of bare@SP displayed the hydrophobic surface with the contact angle nearly of 90º (~ 87º). In contrast, GO coated on WE, GO@SP, presented the hydrophilic surface. The measurement of contact angle of GO@SP was 55º. For HAp-GO@SP, the composition of HAp particles into GO layer could reduce the contact angle to ~ 28º. The decreased contact angle of HAp-GO@SP was due to the increase of porosity and roughness of modified surface [19, 20].

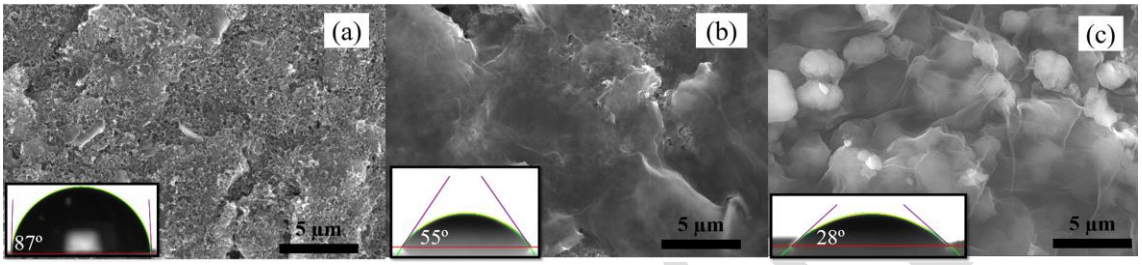

Figure 1 SEM analysis of (a) bare@SP, (b) GO@SP and (c) HAp-GO/SP at surface electrode (WE). Insets are the contact angle of 1 µL of DI water drop on the samples.

3.2 Electrochemical active surface area (ESA) of electrode by cyclic voltammetry

The ESA of bare@SP, GO@SP and HAp-GO@SP were explored in 10 mM $K_3Fe[(CN)_6]$ with 0.1 M KCl as supporting electrolyte. The physicochemical surfaces regarding ion exchange were monitoring via cyclic voltammetry (CV). CV of different electrodes revealed the redox reaction of ferricyanide ion as following chemical reaction (1) [21].

$$[Fe(CN_6)]^{-4} \rightleftharpoons [Fe(CN_6)]^{-3} + e^- \quad (1)$$

The CV of bare@SP (Figure 2 (a)) showed clear redox peaks of ferricyanide ion, whereas both of GO@SP and HAp-GO@SP showed low intensity of redox peaks due to repulsive force between negative charge of functional group on GO surface and ferricyanide ion as shown in Figures 2 (b-c), which was agreement with previous report [14]. Although HAp-GO@SP contained negative charge on its surface, redox peak current was still higher than SP@bare. This occurrence revealed that microcavity of HAp increased ESA for charge transfer on electrode surface. The correlation of oxidation peak current (I, µA) and square root of scan rate ($\upsilon^{1/2}$, $(V \cdot s^{-1})^{-1/2}$) in Figure 2 (d) showed the linear equation of bare@SP, GO@SP and HAp-GO@SP found to be $I = 81.201\ \upsilon^{1/2} + 13.552$ ($R^2 = 0.99144$), $I = 25.932\ \upsilon^{1/2} + 1.285$ ($R^2 = 0.97174$) and $I = 40.454\ \upsilon^{1/2} + 0.660$ ($R^2 = 0.99912$), respectively. For determination of ESA, Randle-Sevcik equation for reversible process at room temperature of 298 K is examined by following equation [10]:

$$I = (2.69 \times 10^5)\, n^{3/2} A D^{1/2} \upsilon^{1/2} C \quad (2)$$

In Eq. (2), I apply to peak current (μA), n is number of electron transfer in redox reaction =1, *A* is ESA (cm^2), D is diffusion coefficient of ferricyanide [22] = 7.6×10^6 cm^2 s^{-1}, υ is the scan rate and C is concentration of ferricyanide = 10 mM. The ESA was calculated from slope of I versus $\upsilon^{1/2}$. The ESA of bare@SP, GO@SP and HAp-GO@SP were estimated to be 10.965×10^{-3}, 3.502×10^{-3} and 5.463×10^{-3} cm^2.

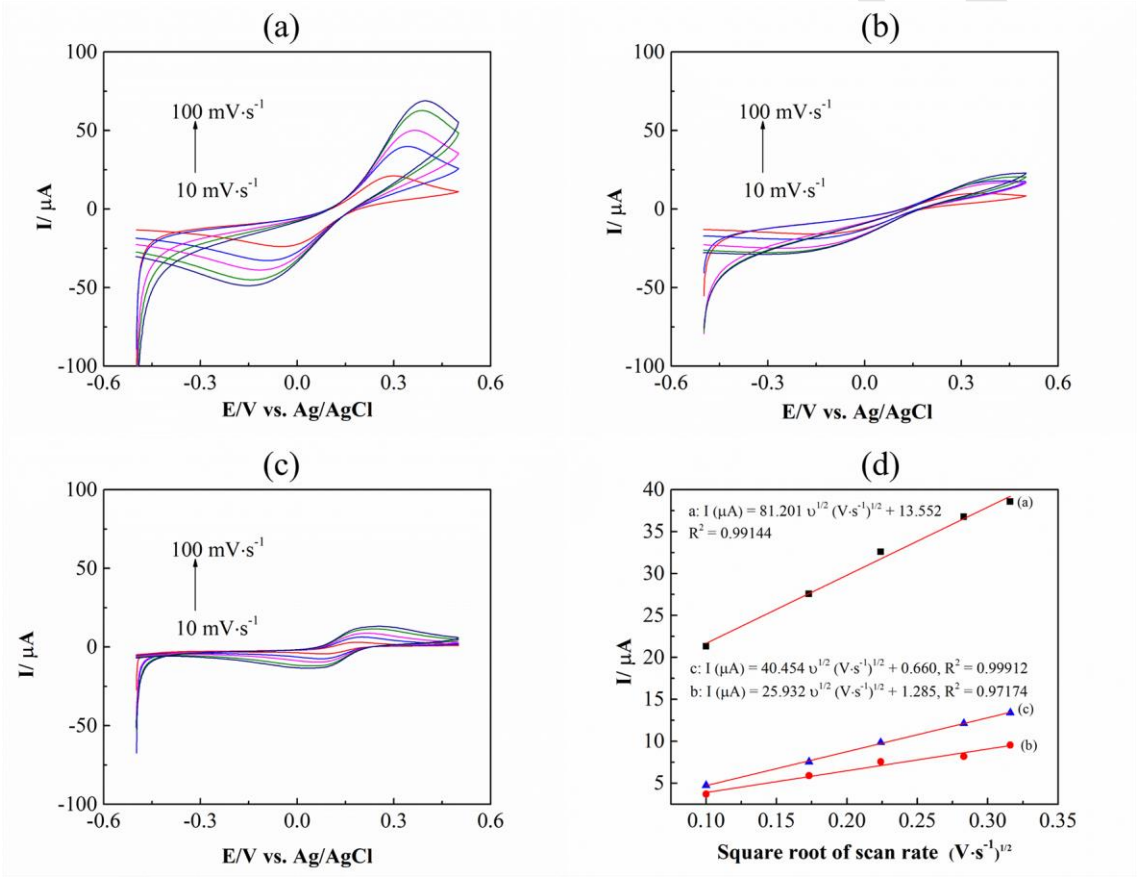

Figure 2 (a) CV of bare@SP, (b) CV of GO@SP and (c) CV of HAp-GO@SP in 10 mM $K_3[Fe(CN)_6]$ in 0.1 M KCl. (d) is plots of I versus square root of scan rate of samples.

3.3 Electrochemical active surface area (ESA) of electrode by chronoamperometry

Chroamperometry (CH-AMP) showed the decreased current versus elapsed time in Figure 3 (a). The physicochemical surfaces from CH-AMP related to oxidation reaction of ferricyanide ion on electrode surface. The decreasing current of bare@SP, GO@SP and

HAp-GO@SP were due to lack of concentration of $[Fe(CN_6)]^{-4}$,which was oxidized to $[Fe(CN_6)]^{-3}$ at fixed applied potential of 0.27 V. The diminishing of initial electroactive concentration enhanced the thickness of diffusion layer that effect to decline of current in I versus time [10]. Afterward, the ESA of these electrodes was evaluated in accordance with the following Cottrel equation [10].

$$I = nFAD^{1/2} C \pi^{1/2} t^{1/2} \quad (3)$$

In Eq. (3), I is current (μA), F is faradaic constant = 96,485 A s mol^{-1}, π is mathematical constant = 22/7, t is elapsed time (s) and other symbols are the same with the equation 1. From linear equation in Figure 3 (b), the relationship between current and inverse of square root of time of bare@SP, GO@SP and HAp-GO@SP were computed to be $I = 1.219\ t^{-1/2} + 0.359$ ($R^2 = 0.91966$), $I = 0.643\ t^{-1/2} + 0.009$ ($R^2 = 0.86743$) and $I = 0.877\ t^{-1/2} + 0.012$ ($R^2 = 0.83519$). Thus, the slope of I against $t^{-1/2}$ were calculated for ESA. The ESA of bare@SP, GO@SP and HAp-GO@SP were estimated to be 0.800×10^{-3}, 0.419×10^{-3} and 0.584×10^{-3} cm^2.

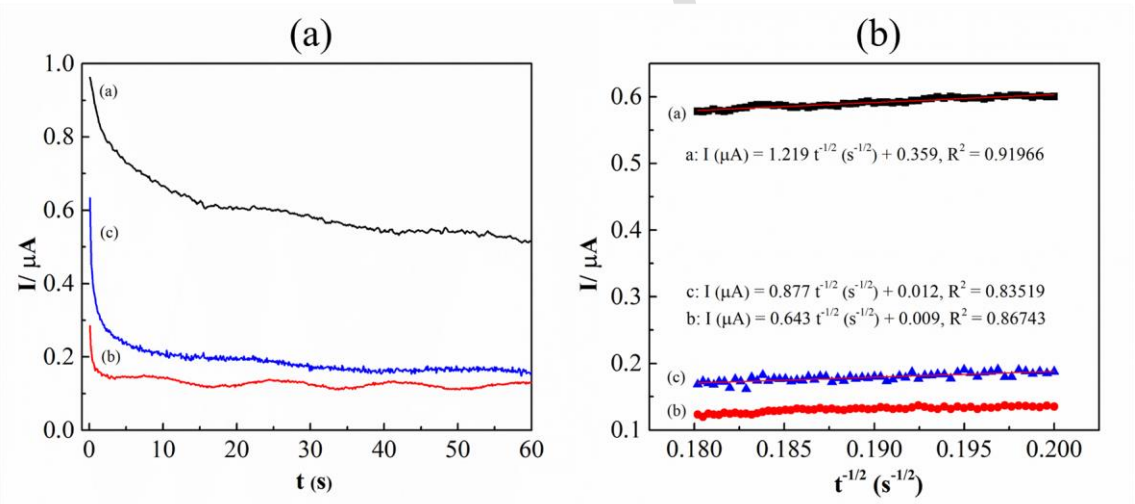

Figure 3 (a, left) chronoamperometry response of (a) bare@SP, (b) GO@SP and (c) HAp-GO@SP in 10 mM $K_3[Fe(CN)_6]$ in 0.1 M KCl. (b, right) was plots of I against $t^{-1/2}$ of the samples.

3.4 Electrochemical active surface area (ESA) of electrode by chronocoulometry

Chronocoulometry (CH-COU) displayed a plot of charge versus time in Figure 4 (a). The physicochemical surfaces from CH-COU inferred adsorption of ferricyanide ion on electrode surface. The steep slope of bare@SP suggested excellent ferricyanide ion adsorbed onto electrode interface, whereas both of GO@SP and HAp-GO@SP showed gradual slope due to anti-charge between ferricyanide ion and electrode surface. These

results were in agreement with results from CV experiments. The ESA of different electrodes was determined by slope of a plot of charge versus square root of time as shown in Figure 4 (b). The ESA was obtained by equation given by Anson [17].

$$Q = 2nFAD^{1/2} C \pi^{-1/2} t^{1/2} + Q_d + Q_{ad} \quad (4)$$

In Eq. (4), Q is charge (μC), Q_d is charges of electrochemical double layer, Q_{ad} is Faradaic charges, which refer to oxidation reaction of $[Fe(CN_6)]^{-4}$ onto electrode surface and other symbols are the same with the equation 1 and 2. The linear equation between charge and square root of time of bare@SP, GO@SP and HAp-GO@SP were computed to be $Q = 0.638\ t^{1/2} - 0.148$ ($R^2 = 0.98489$), $Q = 0.316\ t^{1/2} - 0.052$ ($R^2 = 0.99982$) and $Q = 0.372\ t^{1/2} - 0.069$ ($R^2 = 0.99802$). Next, the slope of Q against $t^{1/2}$ was calculated for ESA. The ESA of bare@SP, GO@SP and HAp-GO@SP were estimated to be 0.213×10^{-3}, 0.105×10^{-3} and 0.124×10^{-3} cm^2, respectively. The tendency of ESA was similar to CV and CH-AMP.

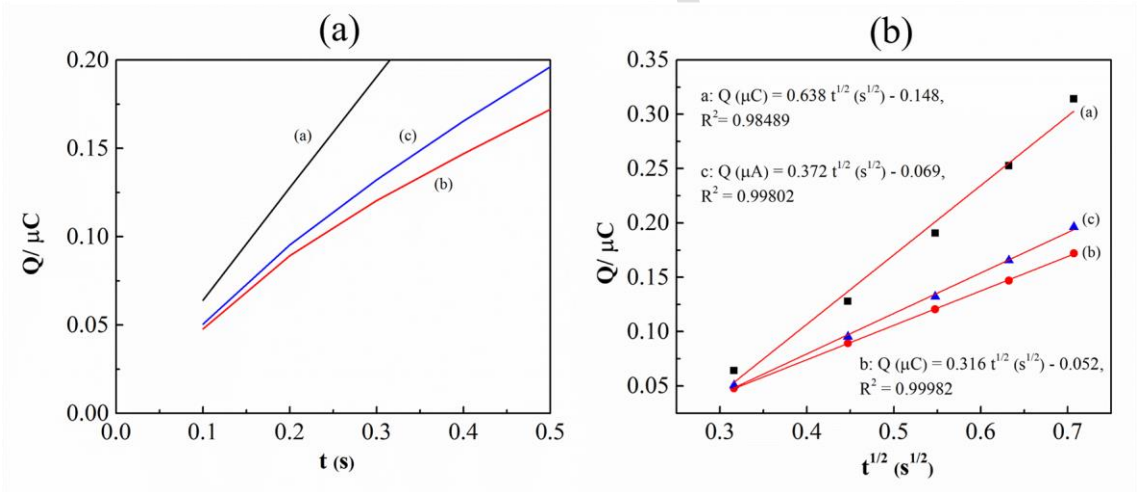

Figure 4 (a, left) chronocoulometry response of (a) bare@SP, (b) GO@SP and (c) HAp-GO@SP in 10 mM $K_3[Fe(CN)_6]$ in 0.1 M KCl. (b, right) is plots of Q against $t^{1/2}$ of the samples.

3.5 Comparison effect of physicochemical surface to ESA determination via CV, CH-AMP and CH-COU

In this study, the physicochemical surface along with wettability and ion exchange of each electrode presented individual properties. For wettability, bare@SP presented hydrophobic surface and both GO@SP and HAp-GO@SP displayed hydrophilic surface.

To compare GO@SP and HAp-GO@SP, contact angle of HAp-GO@SP was lower than GO@SP because the roughness and porosity of HAp increased the physical surface area of HAp-GO@SP to expand adsorption of water. Furthermore, types of charge of electroactive species and types of charge on electrode surface were the major factor to measure ESA. CV was based on collection ion exchange in redox reaction of ferricyanide ion from sweep-potential, whereas CH-AMP and CH-COU were dependent on fixed applied potential. Thus, the robust intensity of current in CV provided highest ESA value from calculation. Although CH-COU presented lowest value of ESA among these techniques, it was necessary to discover interaction of analytical species and electrode interface. In case of absorption form CH-COU, bare@SP could extremely store ferricyanide ion on WE surface. On the other hand, ferricyanide ion could not adsorb on both of GO@SP and HAp-GO@SP because of electrostatic repulsive force of negative charge from both of ferricyanide ion and electrode surface. However, high physical active surface area of HAp in HAp-GO@SP improved ESA to adsorb ferricyanide ion. Thus, ESA of HAp-GO@SP was higher than GO@SP from CH-COU.

4. Conclusion

Three different screen-printed electrodes including bare@SP, GO@SP and HAp-GO@SP were inspected electrochemical active surface area (ESA). From different electrochemical techniques to evaluate ESA, CV provided high value of ESA than CH-AMP and CH-COU, respectively. The physicochemical properties of each electrode were main factor to determine ESA value. Thus, ESA of bare@SP was higher than HAp-GO@SP and GO@SP, respectively. The results form CV, CH-AMP and CH-COU revealed same tendency as those mentioned above. From this knowledge, it might be beneficial to study ESA of materials in electrolyte contained negative charge and be concept to measure ESA of material in electrolyte contained positive charge.

Acknowledgement

We would like to thank the Science Achievement Scholarship of Thailand (SAST) for providing funded Ph.D. to Worapot Prongmanee and Thailand Center of Excellence in Physics (ThEP Center) and National Research Council of Thailand (NRCT) for supporting with research fund.

References

[1] Dupont Madeleine, Hollenkamp Anthony F and Donne Scott W. (2013). Electrochemically active surface area effects on the performance of manganese dioxide for electrochemical capacitor applications. **Electrochimica Acta**, Vol.104. : 140-147.

[2] Juodkazytė J, Šebeka B, Savickaja I, Selskis A, Jasulaitienė V and Kalinauskas P. (2013). Evaluation of electrochemically active surface area of photosensitive copper

oxide nanostructures with extremely high surface roughness. **Electrochimica Acta**. Vol.98. : 109-115.

[3] Reid O'Rian, Saleh Farhana S. and Easton E. Bradley. (2013). Determining electrochemically active surface area in PEM fuel cell electrodes with electrochemical impedance spectroscopy and its application to catalyst durability. **Electrochimica Acta**. Vol.114. : 278-284.

[4] Torija Sergio, Prieto-Sanchez Laura and Ashton Sean J. (2016). In-situ electrochemically active surface area evaluation of an open-cathode polymer electrolyte membrane fuel cell stack. **Journal of Power Sources**. Vol.327. : 543-547.

[5] Worapot Prongmanee, Ibrar Alam and Piyapong Asanithi. (2019). Hydroxyapatite/Graphene oxide composite for electrochemical detection of L-Tryptophan. **Journal of the Taiwan Institute of Chemical Engineers** Vol.102. : 415-423.

[6] Aldana-González J, Olvera-García J, Montes de Oca M G, Romero-Romo M, Ramírez-Silva M T and Palomar-Pardavé M. (2015). Electrochemical quantification of the electro-active surface area of Au nanoparticles supported onto an ITO electrode by means of Cu upd. **Electrochemistry Communications**. Vol.56. : 70-74.

[7] Lukaszewski M, Soszko M and Czerwinski A. (2016). Electrochemical Methods of Real Surface Area Determination of Noble Metal Electrodes - an Overview. **International Journal of Electrochemical Science**. Vol.11. Issue 6. : 4442-4469.

[8] McCrum Ian T and Janik Michael J. (2017). Deconvoluting Cyclic Voltammograms To Accurately Calculate Pt Electrochemically Active Surface Area. **The Journal of Physical Chemistry C**. Vol.121. Issue 11. : 6237-6245

[9] Pfaffmann Lukas, Birkenmaier Claudia, Müller Marcus, Bauer Werner, Mitsch Tim, Feinauer Julian, Krämer Yvonne, Scheiba Frieder, Hintennach Andreas, Schleid Thomas, Schmidt Volker and Ehrenberg Helmut. (2016). Investigation of the electrochemically active surface area and lithium diffusion in graphite anodes by a novel OsO4 staining method. **Journal of Power Sources**. Vol.307. : 762-771.

[10] Wang Joseph. (2006). **Analytical Electrochemistry**. Edition 3. USA: John Wiley & Sons.

[11] Shetti Nagaraj P, Nayak Deepti S, Malode Shweta J and Kulkarni Raviraj M. (2017). Electrochemical Sensor Based upon Ruthenium Doped TiO2 Nanoparticles for the Determination of Flufenamic Acid. **Journal of The Electrochemical Society**. Vol.164. Issue 5. : B3036-B3042.

[12] Shetti Nagaraj P, Nayak Deepti S, Malode Shweta J and Kulkarni Raviraj M. (2017). An electrochemical sensor for clozapine at ruthenium doped TiO2 nanoparticles modified electrode. **Sensors and Actuators B: Chemical**. Vol.247. : 858-867.

[13] Nayak Deepti S and Shetti Nagaraj P. (2016). A novel sensor for a food dye erythrosine at glucose modified electrode. **Sensors and Actuators B: Chemical**. Vol.230. :140-148.

[14] Gao Feng, Cai Xili, Wang Xia, Gao Cai, Liu Shaoli, Gao Fei and Wang Qingxiang. (2013). Highly sensitive and selective detection of dopamine in the presence of ascorbic acid at graphene oxide modified electrode. **Sensors and Actuators B: Chemical**. Vol.186. : 380-387.

[15] Li Junhua, Kuang Daizhi, Feng Yonglan, Zhang Fuxing, Xu Zhifeng, Liu Mengqin and Wang Deping. (2013). Electrochemical tyrosine sensor based on a glassy carbon electrode modified with a nanohybrid made from graphene oxide and multiwalled carbon nanotubes. **Microchimica Acta**. Vol.180. Issue 1. : 49-58

[16] Wang Shiqiao, Zhai Haiyun, Chen Zuanguang, Wang Haihang, Tan Xuecai, Sun Guohan and Zhou Qing. (2017). Constructing a Sensitive Electrochemical Sensor for Tyrosine Based on Graphene Oxide-ε-MnO2 Microspheres/Chitosan Modified Activated Glassy Carbon Electrode. **Journal of The Electrochemical Society**. Vol.164. Issue 14. : B758-B766.

[17] Anson Fred C and Osteryoung Robert A. (1983). Chronocoulometry: A convenient, rapid and reliable technique for detection and determination of adsorbed reactants. **Journal of Chemical Education**. Vol.60. Issue 4. :293.

[18] Mazzaracchio Vincenzo, Tomei Maria Rita, Cacciotti Ilaria, Chiodoni Angelica, Novara Chiara, Castellino Micaela, Scordo Giorgio, Amine Aziz, Moscone Danila and Arduini Fabiana. (2019). Inside the different types of carbon black as nanomodifiers for screen-printed electrodes. **Electrochimica Acta**. Vol.317. : 673-683.

[19] Song Shuang, Yang Hao, Su Chunping, Jiang Zhibin and Lu Zhong. (2016). Ultrasonic-microwave assisted synthesis of stable reduced graphene oxide modified melamine foam with superhydrophobicity and high oil adsorption capacities. **Chemical Engineering Journal**. Vol.306. : 504-511.

[20] Song Shuang, Yang Hao, Zhou Cailong, Cheng Jiang, Jiang Zhibin, Lu Zhong and Miao Jing. (2017). Underwater superoleophobic mesh based on $BiVO_4$ nanoparticles with sunlight-driven self-cleaning property for oil/water separation. **Chemical Engineering Journal**. Vol.320. : 342-351.

[21] Mortimer, R. J. (1999). **Encyclopedia of Spectroscopy and Spectrometry**. Edition 1. Oxford: Elsevier.

[22] Dağcı Kader and Alanyalıoğlu Murat. (2016). Preparation of Free-Standing and Flexible Graphene/Ag Nanoparticles/Poly(pyronin Y) Hybrid Paper Electrode for Amperometric Determination of Nitrite. **ACS Applied Materials & Interfaces**. Vol.8. Issue 4. : 2713-2722.

Dr. Piyapong Asanithi is Associate Professor of Physics, Department of Physics, King Mongkut's University of Technology Thonburi, Thailand He did his B.Sc. from Department of Physics, Faculty of Science, Narasuan University, Pitsanulok, Thailand 2004. He did his Ph.D. degree from Department of Physics, University of Surrey, Guildford, UK, 2010. His research inserts are synthesis of low-dimensional materials and bio-related materials and fabrication and characterization of novel hybrid materials based on low-dimensional materials and bio-related materials. He has distributed more than 20 papers in renowned journals.

Worapot Prongmanee completed his B.Sc. and M.Sc. degree in Department of Physics, Faculty of Science, from King Mongkut's University of Technology Thonburi, Thailand, 2011 and 2013. Presently, he is doing Ph.D. degree in Department of Physics, King Mongkut's University of Technology Thonburi, Thailand. His research is based on electrochemical sensor, metal nanoparticle synthesis, graphene based material synthesis.